Journal of Applied Electrochemistry (2007) 37:95–101
DOI 10.1007/s10800-006-9214-z

Electrochemical studies on Sr doped $LaMnO_3$ and $LaCoO_3$ layers synthesised in a low-pressure plasma reactor equipped with a convergent nozzle

FRÉDÉRIC ROUSSEAU, MEHRDAD NIKRAVECH*, LINDA BENABDELMOUMÈNE, CÉDRIC GUYON, DANIEL MORVAN and JACQUES AMOUROUX
Laboratoire de Génie des Procédés Plasmas et Traitements de Surfaces (ENSCP-Pierre et Marie Curie University), ENSCP, 11 rue Pierre et Marie Curie, 75005, Paris, France
*(*author for correspondence, tel.: + 33-01-46-33-42-83, e-mail: mehrdad-nikravech@enscp.fr)*

Received 14 February 2006; accepted in revised form 13 June 2006

Key words: catalysis, Faradaic impedance, impedance spectroscopy, low-pressure plasma, perovskite, Solid Oxide Fuel Cell (SOFC) cathode

Abstract

The aim of this work was to synthesise and deposit a perovskite ($La_{1-x}Sr_xMnO_3$ or $La_{1-x}Sr_xCoO_3$) cathode on an SOFC electrolyte (8% Yttria Stabilised Zirconia – YSZ). The recombination of atomic oxygen on Sr doped $LaMnO_3$ was performed in order to study the properties of perovskite for the adsorption of oxygen. The electrical resistance of the layers was measured as a function of the chemical composition. Impedance measurements on different samples were performed in order to analyse the electrochemical response of the cathode – electrolyte stack as a function of temperature and nature of the atmosphere. Moreover, the Faradaic impedance representing the electrochemical processes at the cathode – electrolyte interface was calculated from the global impedance in various conditions.

1. Introduction

The chemical reactivity, ionic and electrical conductivity of SOFC cathodes depend on their purity, stochiometry and structure, which are functions of the manufacturing process parameters [1]. For example, the usual ways to synthesise ceramic [1–4] as calcination, sol–gel method or carbonate co-precipitation often lead to products containing pollutants. Bell et al. [1] have shown that the presence of undesirable phases in the product decreases the catalytic properties. For example adsorption of O_2 at the cathode surface will be poor. To improve the quality of the deposits and to reduce the costs by integrating the depositing steps into a single process, new production techniques, such as thermal plasma processes, are under development [5–7]. Nevertheless, thermodynamics shows that undesirable phases (La_2O_3, $La(OH)_3$, Mn_3O_4...) could appear at high temperature ($T > 2000$ K) [5–7]. In order to produce SOFC high quality cathodes, a low-pressure plasma reactor has been developed in our laboratory [8–10].

The raw material (lanthanum nitrates, manganese nitrates, cobalt nitrates or strontium nitrates dissolved in water) is injected into the plasma reactor in order to obtain a cathode layer on YSZ pellets (19 mm in diameter). Recent work allowed optimisation of the process by investigating different synthesis parameters [8–10]. Scanning Electron Microscopy (SEM) was performed to study the quality and the structure of the layers deposited. The SOFC cathode must have a high electronic conductivity and good catalytic activity to allow the reduction of O_2 to O^{2-} [11, 12].

2. Description of the low-pressure plasma process

2.1. *Experimental Set-up*

The low-pressure plasma process is described on Figure 1. The plasma reactor consists of a quartz tube (46 mm in internal diameter, 600 mm in length) equipped with a convergent nozzle (5 or 3 mm in diameter). A 40 MHz RF generator was used to initialise and maintain the plasma discharge by means of six inductive coils located on the nozzle (available power in the plasma = 100–400 W). Mixtures of argon and oxygen in various ratio were used as plasma gases (maximum flow 1.66 $cm^3\ min^{-1}$). Mass flow-meters were used to control the composition, the flow and the pressure of the plasma and vector gases. A vacuum pump permitted the pressure in the reactor to be maintained within a range of 60–600 Pa (at the exit of the nozzle) [8–10].

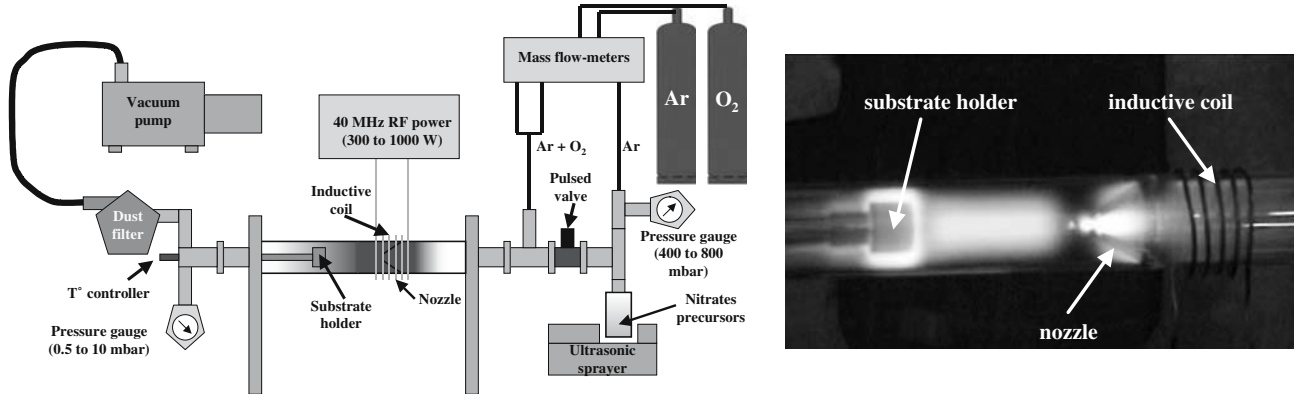

Fig. 1. Plasma process experimental set-up.

The raw material was a mixture of La, Mn, Sr or Co nitrates dissolved in water (ICP- DCP standard solution – ALDRICH). The composition of the mixture was calculated according to the stochiometry of the layer needed for a perovskite composite on YSZ substrate (YSZ 8% CERAC). An ultrasonic sprayer was used to produce fine droplets of liquid precursors (10 μm in diameter) at the head of the reactor. The sprayer was insulated from the reactor by means of a pulsed valve. Pressure levels before the valve ranged from 5×10^4 to $4 \times 10-4$ Pa. During the pulsed valve opening time (usually 0.25 s opening and 5 s closing), nitrate droplets went through the plasma and reacted with the oxidant species ($O^{\cdot}$ and OH radicals), leading to the destruction of the NO_3 bond and the formation of La–O, Sr–O, Mn–O or Co–O bond. Finally, after passing through the plasma reactor, particles deposited on the YSZ substrate in order to form Sr-doped $LaMnO_3$ or $LaCoO_3$ amorphous layers. The deposit thus grew into a layer 40–50 μm h^{-1} thick. Because of the convergent nozzle, over-pressure waves were created, leading to the acceleration of the gases and particles circulating in the reactor [8–10]. The high velocity of the micrometric particles (80 m s^{-1} measured by Laser Doppler Anemometry at the exit of the nozzle) led to a very strong adherence of the cathode layer on the YSZ substrate.

2.2. *Appearance of the layers*

Scanning Electron Microscopy (SEM), Electron Diffraction Scanning (EDS) and X-ray diffraction (XRD) were used to study the structure and composition of the coatings. EDS showed that the chemical composition of the layer corresponded to the stochiometry of the nitrate solution. Moreover, X-ray diffraction patterns demonstrated that coatings annealed at 750 °C for 1 h gave a single phase perovskite structure. No undesirable phases such as La_2O or $La(OH)_3$ were observed on X-ray diagrams.

Scanning electron microscopy was used to observe the structure and porosity of the layers deposited. Figure 2(a) shows that the surface of $LaMnO_3$ layers is porous and made up of agglomerated particles. The layers are relatively amorphous (XRD), due to the low temperature in the plasma reactor. In order to crystallise the deposit, it is necessary to anneal it at high temperature (700–1200 °C). The deposit shown on Figure 2(a) was annealed at 1200 °C for 1 h. SEM observations after the annealing (Figure 2(b)) underline the transition from an amorphous structure to an orderly structure due to the high temperature (confirmed by XRD).

Figure 3 shows the fractured cross section of $LaMnO_3$ layers on YSZ annealed at 750 °C. The bulk of the layers is shown to be porous. Scratching the coating with a scalpel confirms that the layers adhere strongly to the electrolyte. The influence of doping elements was studied by the addition of Sr nitrates to the starting solution. Deposits of Sr-doped $LaMnO_3$ exhibit the same structure and the same adherence. $LaCoO_3$ layers have the same structure as $La_{1-x}Sr_xMnO_3$ ones, but lanthanum cobaltites doped with strontium atoms

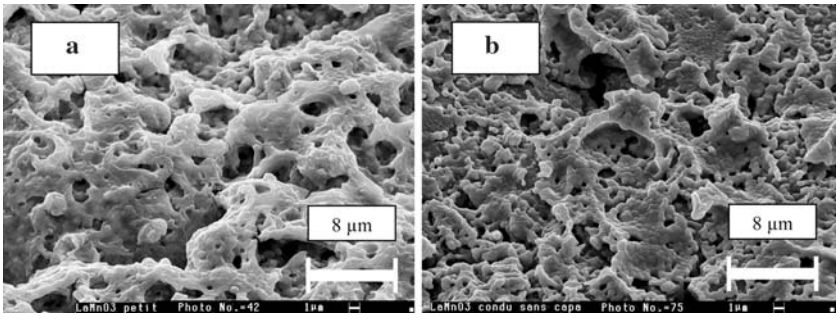

Fig. 2. $LaMnO_3$ layers just after the synthesis (a) and after an annealing at 1200 °C during 1 h (b).

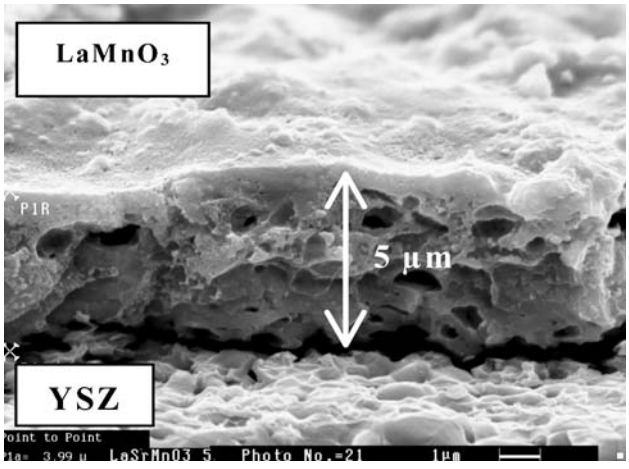

Fig. 3. Fractured cross section of Lanthanum manganite deposited on YSZ (after annealing at 750 °C for 1 h).

($La_{0.7}Sr_{0.3}CoO_3$) exhibit a hexagonal structure after annealing as shown in Figure 4.

3. Electrochemical studies of Sr-doped $LaMnO_3$ and $LaCoO_3$ layers

The efficiency of an SOFC depends strongly on the cathode properties. Cathode layers must permit the adsorption and the dissociation of molecular oxygen into two O^- [11, 12]. O^- diffuses on the surface of lanthanum manganites and reacts at the cathode/electrolyte interface to produce O^{2-}. Finally, O^{2-} is incorporated and diffuses in the bulk of YSZ (electrochemical engine of the cell). Because the layer properties depend on the synthesis process [1], it was essential to study the electrical and catalytic properties of the coatings deposited on YSZ samples.

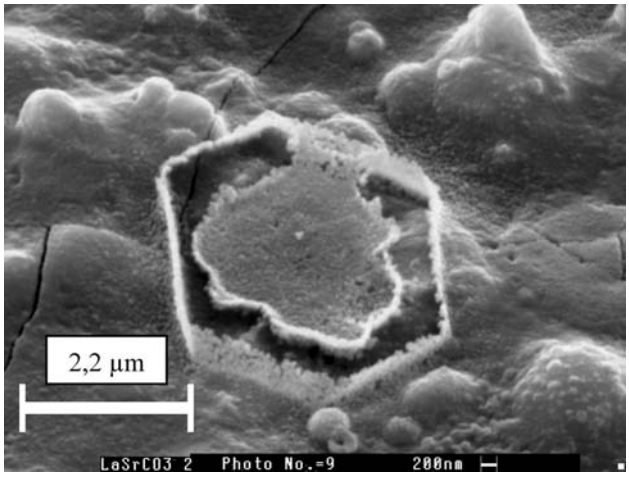

Fig. 4. Hexagonal structure on the surface of $La_{0.7}Sr_{0.3}CoO_3$ annealed at 600 °C for 46 h.

3.1. *Investigations about the adsorption of oxygen on the surface of $La_{0.7}Sr_{0.3}MnO_3$*

The efficiency of a catalyst depends on its composition, which determines the activation energy and number of active sites for chemical reaction [13]. In this study, a measurement of the atomic oxygen recombination coefficient γ was performed on the $La_{0.7}Sr_{0.3}MnO_3$ (LSM) surface, in order to estimate the activation energy and the number of sites for oxygen adsorption.

LSM was deposited on a YSZ sample (25 mm in diameter) and annealed at 750 °C for 1 h. Then the LSM/YSZ stack was placed in a low-pressure plasma reactor developed for the study of atomic oxygen recombination for several materials [13, 14]. The recombination coefficient was calculated using the actinometry spectroscopic method. The principle of actinometry consists in measuring the intensity ratios of excited species of oxygen on excited species of argon added to the plasma in small quantities. The oxygen atoms concentration was monitored with optical emission from O (844.6 nm) and Ar (811.5 nm). The ratio I_O/I_{Ar} is related to the concentration ratio by the following equation:

$$I_O/I_{Ar} = k[(O)/(Ar)] \tag{1}$$

The recombination coefficient γ was deduced from the following equation and was calculated from the atomic oxygen concentration profile along the reactor:

$$\gamma = \frac{-4D\nabla(I_O/I_A)_x}{c[-\nabla(I_O/I_A)_x L + (I_O/I_A)_0]} \tag{2}$$

where D is the binary coefficient ($m^2\ s^{-1}$), c the atomic velocity ($m\ s^{-1}$), L the width of the boundary layer (m), $\nabla(I_O/I_{Ar})_x$ the axial concentration gradient and $(I_O/I_{Ar})_0$ the steady state ratio (out of the boundary layer).

Equation (2) describes the movement of oxygen atoms in the boundary layer near the sample. The recombination coefficient is linked to the surface temperature by the following equation:

$$\gamma = \frac{C_a h^2/2\pi m_O k}{T} \exp\left(-\frac{E_a}{RT}\right) \tag{3}$$

where E_a is the activation energy of the surface reaction ($J\ mol^{-1}$), C_a the number of active sites (atoms m^{-2}) and m_O the mass of an oxygen atom (kg). The activation energy of the process and the number of active sites corresponding to LSM could be deduced by calculating γ using Equation (2) (Figure 5) and by plotting $\ln(\gamma T)$ as a function of $1/T$ as shown in Figure 6. The activation energy for the recombination of oxygen was calculated to be 6.3 kJ mol^{-1} ± 15% by using Equation (3). The number of active sites was estimated at around 1.7×10^{20} atoms m^{-2} ± 15%. Results show that LSM deposited on YSZ by the plasma process presents a significant catalytic activity for oxygen adsorption.

Further investigations will consist in studying the effect of an increase in temperature on the activation

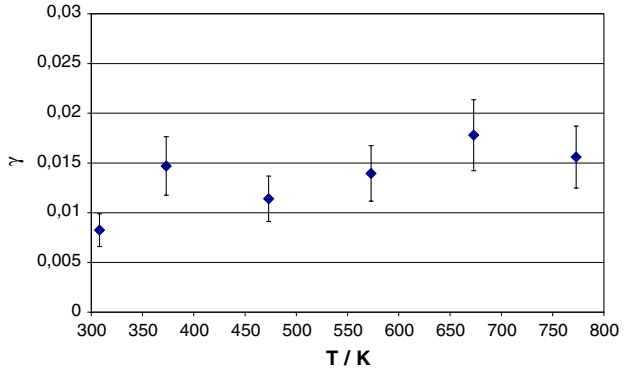

Fig. 5. Evolution of recombination coefficient γ as a function of temperature.

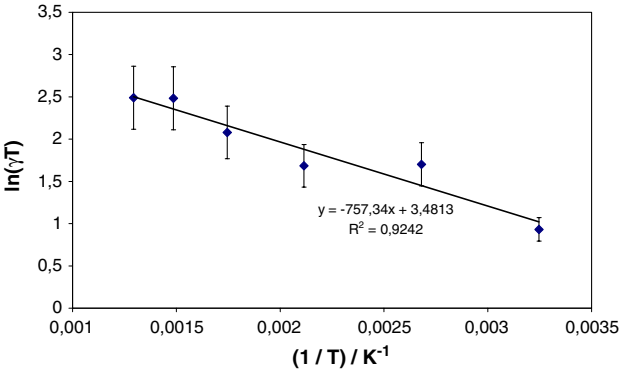

Fig. 6. Evolution of $\ln(\gamma T)$ as a function of $1/T$ (activation energy and number of active sites).

energy and the number of active sites ($T > 500$ °C). Moreover, a comparison of γ for several materials will be performed to study what role stochiometry, plasma parameters and annealing play on adsorption properties.

3.2. *Impedance spectroscopy*

Impedance measurements were carried out in open circuit conditions in air or in N_2 atmosphere at different temperatures. In the case of cathodes deposited on YSZ, the first reference electrode and the counter electrode were applied to the YSZ with a Pt mesh. The working electrode and the second reference electrode were connected to the cathode side with a Pt disk. A spring permitted to apply a constant force on the electrodes on both sides of the cell. The complex impedance measurements were made over frequencies ranging from 65535 to 1 Hz with a SOLARTRON Frequency Response Analyser 1250, a potentiostat SI 1287 and a computer equipped with Z-Plot software. Recent impedance measurements proved that the impedance of the layers stabilises to a constant value after two 1 h annealing processes at 750 °C.

The results presented in Figures 7–9 exhibit the behaviour of the layers under various conditions of temperature and atmosphere. The response of YSZ pellets with an $La_{0.7}Sr_{0.3}MnO_3$ deposit (LSM/YSZ) may be compared with that of YSZ pellets only. It can be observed that:

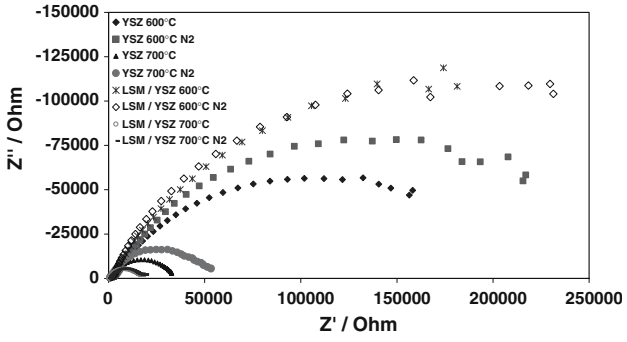

Fig. 7. Global impedance plots of YSZ and YSZ/$La_{0.7}Sr_{0.3}MnO_3$ stack measured in air and N_2 at 600 and 700 °C.

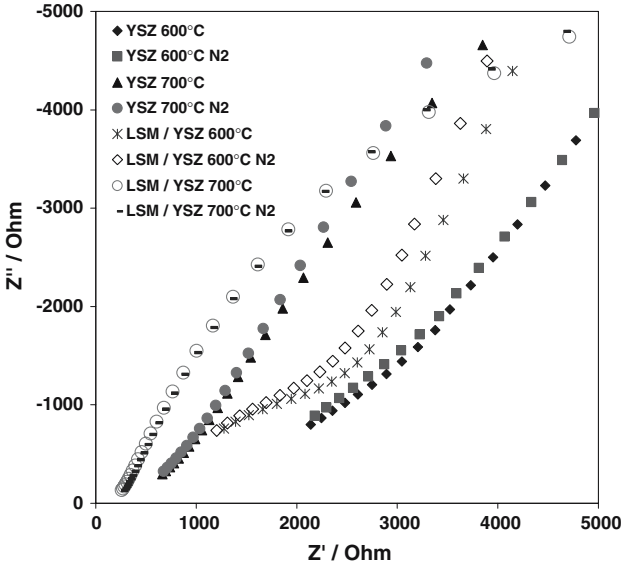

Fig. 8. Global impedance plots of YSZ and YSZ/$La_{0.7}Sr_{0.3}MnO_3$ stack measured in air and N_2 at 600 and 700 °C, zoom from 0 to 5000 Ω.

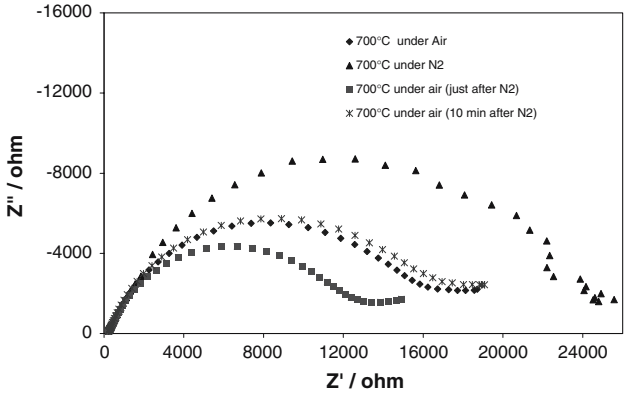

Fig. 9. Global impedance plots of YSZ/$La_{0.7}Sr_{0.3}MnO_3$ stack measured in air and N_2 at 700 °C, zoom from 0 to 26,000 Ω.

1. The real part resistance of LSM/YSZ in air lowers from 3.5×10^5 Ω down to 1.7×10^4 Ω when the temperature increases from 600 to 700 °C (Figure 7).
2. At high frequency values, the complex plots exhibit an additional semicircle at low temperature, which could be due to Pt electrodes (Figure 8).
3. The LSM/YSZ stack exhibits a higher real part resistance than YSZ alone at the lower temperature (600 °C), while the opposite behaviour is noticed at 700 °C (Figure 7).
4. The Pt electrodes seem to participate in the oxygen transfer between air and YSZ, which could explain the conductivity of YSZ alone. In Figure 7, the increase in the real part resistance at 600 °C is due to the presence of LSM on the YSZ surface. At low temperature, LSM does not allow the transfer of oxygen at the interface. However, at 700 °C, the real part resistance of LSM/YSZ becomes lower than that of YSZ alone. At high temperature, the contribution of LSM activity to oxygen transfer enhances the global conductivity of the LSM/YSZ stack as expected.
5. The presence of oxygen plays a major role on the real part resistance of the layers. YSZ in air exhibits a lower resistance than under N_2 atmosphere, which can be explained by the diffusion of oxygen from Pt electrodes. The behaviour of LSM/YSZ at 600 °C does not exhibit any noticeable change with and without oxygen (Figure 7). This shows that at low temperature, the chemical activity of LSM is low enough to create a barrier to oxygen transfer between the Pt electrodes and YSZ. In Figure 9, the real part resistance of LSM/YSZ is lower with the presence of oxygen at 700 °C. This underlines the chemical activity of LSM for oxygen transfer at high temperature.
6. The results show that YSZ and LSM/YSZ stack present electrochemical responses for oxygen (Figures 7 and 9). The LSM chemical activity for oxygen transfer changes drastically for an increase in temperature from 600 to 700 °C.

3.3. *Calculation of Faradaic impedance*

It is often assumed that the global impedance of the LSM/YSZ stack depends on electrochemical processes as well as on other electrical phenomena. The Faradaic impedance (Z_f) representing the electrochemical processes at the interface can be separated from the global impedance by a method developed by Berthier et al. [15]. Mitterdorfer and Gauckler [16] used this method to study the LSM/YSZ interface. From Z_f, they determined different resistances (Figure 10): a charge transfer resistance (R_t) due to the transfer of oxygen ions at the LSM/YSZ interface, a concentration resistance (R_c) due to the diffusion of oxygen at the LSM surface and finally a polarisation resistance (R_p). In the case studied, the Faradaic impedance was calculated from the impedance spectra at 600 and 750 °C as shown in Figure 11.

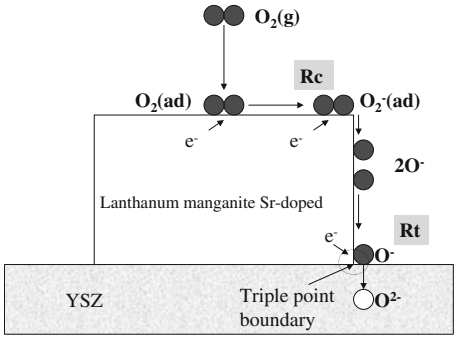

Fig. 10. Mechanism of oxygen transfer into YSZ [11, 12, 16].

Results showed that the Faradaic impedance could not be separated from the global impedance at $T = 600$ °C; this may be due to the absence of transfer of oxygen at the interface between LSM and YSZ (Figure 11). The polarisation resistance was only controlled by the concentration resistance (R_c). The results agreed with the impedance measurements performed on LSM/YSZ under air and N_2, the absence of oxygen at 600 °C did not change the complex plots. At 750 °C, it was possible to separate the Faradaic impedance from the global impedance, which may signify that the polarisation resistance of the cell was controlled by the transfer resistance (R_t) and by the concentration resistance (R_c). In other words, the electrochemical process for oxygen transfer is activated at 750 °C in accordance with the observations made in Section 3.2.

Results and calculations underline the fact that the oxygen transfer occurred at temperatures superior to 700 °C. This work proved that the cathode material deposited through a plasma process was sensitive to oxygen. Other impedance measurements should be performed on various materials at high temperature and under high oxygen pressure.

3.4. *Role of the chemical composition*

The resistance properties of the layers, depending on their chemical composition, were studied by measuring the resistance between voltage probes applied on the surface. Three samples with various stochiometry ($La_{0.7}Sr_{0.3}MnO_3$, $LaCoO_3$, $La_{0.7}Sr_{0.3}CoO_3$) were deposited on quartz pellets (19 mm in diameter) in the same plasma conditions.

Figure 12 shows the evolution of the resistance during annealing time at 600 °C. The resistance decreases with time, which is probably due to a change in the crystalline structure. As expected, lanthanum cobaltites exhibit a lower resistance than lanthanum manganites. Doping lanthanum with Sr atoms leads to a more significant decrease in the resistance. It must be noted that the Sr doped layers exhibit the same resistance profile.

Figure 13 shows the resistance of the three annealed deposits as a function of time. The resistance of the

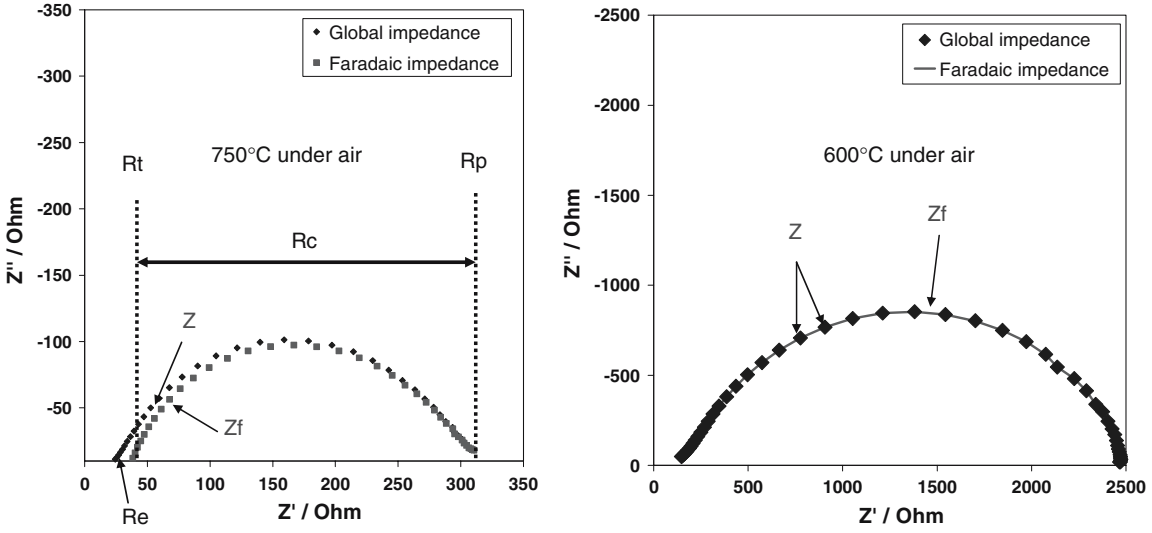

Fig. 11. Global impedance (Z) and Faradaic impedance (Z_f) of $La_{0.7}Sr_{0.3}MnO_3$/YSZ stack measured in air at 600 and 750 °C.

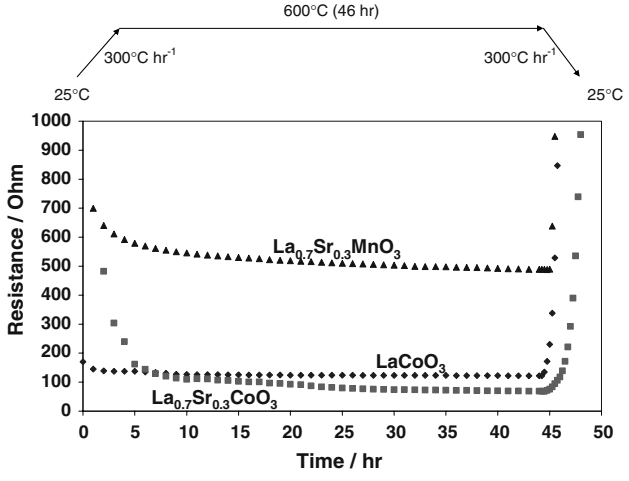

Fig. 12. Effect of annealing on the resistance of deposited layers.

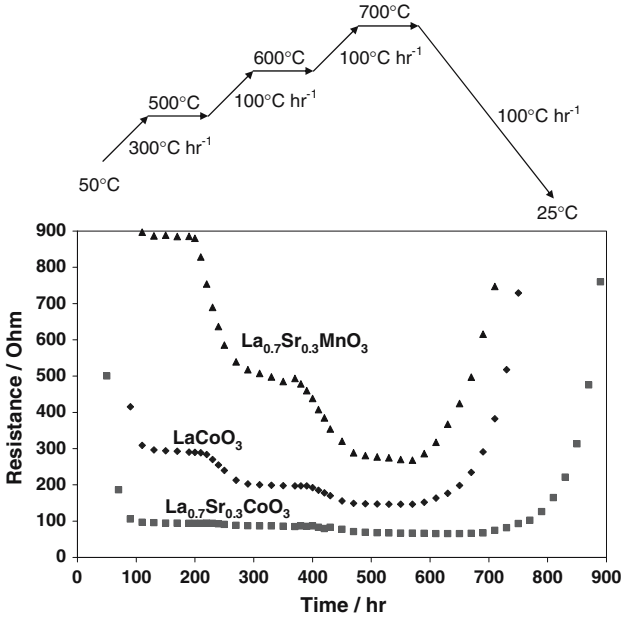

Fig. 13. Resistance of three different deposits vs. time (at 500, 600, 700 °C).

deposits decreases as the temperature increases. The comparison of the layers points out the fact that the lanthanum cobaltites have a lower resistance than lanthanum manganites. Doping the layers with strontium further decreases the resistance.

4. Conclusion

A low-pressure plasma process allows synthesis of high purity cathode layers of various stochiometric levels. The process enables synthesis and deposition of a layer with perovskite structure in one step with accurate control of the parameters. The materials deposited exhibit the necessary porosity and adherence on YSZ necessary for SOFC application. Catalysis and impedance spectroscopy have shown that the deposits are sensitive to oxygen. Resistance measurements at high temperature have proved that doping lanthanum manganites or lanthanum cobaltites with Sr decreases the resistance of the deposit. In this work, it is demonstrated that layers deposited through plasma process could be used as cathode materials for SOFC devices.

References

1. R.J. Bell, G.J. Millar and J. Drennan, *Solid State Ionics* **131** (2000) 211.
2. T. Yamada, N. Chitose, J. Akikusa, N. Murakami, T. Akbay, T. Miyazawa, K. Adachi, A. Hasegawa, M. Yamada, K. Hoshino, K. Hosoi, N. Komada, H. Yoshida, M. Kawano, T. Sasaki, T. Inagaki, K. Miura, T. Ishihara and Y. Takita, *J. Electrochem. Soc.* **151**(10) (2004) 1712.
3. N. Imanishi, T. Matsumura, Y. Sumiya, K. Yoshimura, A. Hirano, Y. Takeda, D. Mori and R. Kanno, *Solid State Ionics* **174** (2004) 245.

4. F.J. Lepe, J. Fernandez-Urban, L. Mestres and M.L. Martinez-Sarrion, *Power Sources* **151** (2005) 74.
5. T. Yoshida, T. Okada, H. Hamatani and H. Kumaoka, *Plasma Sources Sci. Technol.* **1** (1992) 195.
6. G. Schiller, R. Henne and M. Lang, *in* P. Stevens (Ed), 'Third European Solid Oxide Fuel Cell Forum', Proceeding (Nantes, France, 1998), pp. 123–132.
7. C. Monterrubio Badillo, H. Ageorges, T. Chartier, J.F. Coudert and P. Fauchais, *in* P. Fauchais (Ed), 'Progress in Plasma Processing Materials' (Begell House, New York, 2003), pp. 535–541.
8. M. Nikravech, F. Rousseau, D. Morvan and J. Amouroux, *Phys. Chem. Solids* **64** (2003) 1771.
9. M. Nikravech, F. Rousseau, D. Morvan and J. Amouroux, *High Technol. Plasma Process.* **7** (2003) 225.
10. F. Rousseau, M. Nikravech, E. Francke, J. Milpied, D. Morvan and J. Amouroux, *High Technol. Plasma Process.* **8** (2004) 416.
11. T. Horita, K. Yamaji, M. Ishikawa, N. Sakai and H. Yokokawa, *J. Electrochem. Soc.* **145**(9) (2002) 3196.
12. T. Horita, K. Yamaji, N. Sakai, Y. Xiong, T. Kato, H. Yokokawa and T. Kawada, *Appl. Surf. Sci.* **303–304** (2003) 634.
13. C. Guyon, S. Cavadias and J. Amouroux, *Surf. Coat. Technol.* **142–144** (2001) 959.
14. C. Guyon, S. Cavadias, I. Mabille, M. Moscosa-Santillan and J. Amouroux, Catal. Today (2004) 159.
15. F. Berthier, J.P. Diard, B. Le Gorrec and C. Montella, *Sci. Eng. Corros.* **51** (1995) 105.
16. A. Mitterdorfer and L.J. Gauckler, *Solid State Ionics* **111** (1998) 185.